Lawrence Berkeley National Laboratory
LBL Publications

Title
Combined soft and hard X-ray ambient pressure photoelectron spectroscopy studies of semiconductor/electrolyte interfaces

Permalink
https://escholarship.org/uc/item/5ph6278h

Authors
Starr, David E
Favaro, Marco
Abdi, Fatwa F
et al.

Publication Date
2017-11-01

DOI
10.1016/j.elspec.2017.05.003

Peer reviewed

Combined soft and hard X-ray ambient pressure photoelectron spectroscopy studies of semiconductor/electrolyte interfaces

David E. Starr[a,*], Marco Favaro[a,b], Fatwa F. Abdi[a], Hendrik Bluhm[b,c], Ethan J. Crumlin[b], Roel van de Krol[a]

[a]*Institute for Solar Fuels, Helmholtz-Zentrum Berlin für Materialien und Energie GmbH, Hahn-Meitner-Platz 1, 14109 Berlin, Germany*

[b]*Advanced Light Source, Lawrence Berkeley National Laboratory, Berkeley, CA 94720, USA*

[c]*Chemical Sciences Division, Lawrence Berkeley National Laboratory, Berkeley, CA 94720, USA*

Abstract

The development of solar fuel generating materials would greatly benefit from a molecular level understanding of the semiconductor/electrolyte interface and changes in the interface induced by an applied potential and illumination by solar light. Ambient pressure photoelectron spectroscopy techniques with both soft and hard X-rays, AP-XPS and AP-HAXPES respectively, have the potential to markedly contribute to this understanding. In this paper we initially provide two examples of current challenges in solar fuels material development that AP-XPS and AP-HAXPES can directly address. This will be followed by a brief description of the distinguishing and complementary characteristics of soft and hard X-ray AP-XPS and AP-HAXPES and best approaches to achieving monolayer sensitivity in solid/aqueous electrolyte studies. In particular we focus on the detection of adsorbed hydroxyl groups in the presence of aqueous hydroxyls in the electrolyte, a common situation when investigating photoanodes for solar fuel generating applications. The paper concludes by providing an example of a combined AP-XPS and AP-HAXPES study of a semiconductor/aqueous electrolyte interface currently used in water splitting devices specifically the $BiVO_4$/aqueous potassium phosphate electrolyte interface.

Introduction

Due to the intermittency of many forms of renewable energy, such as solar and wind, there is currently a large research effort focusing on understanding and developing electrochemical reactions that can store renewable energy [1]. In this respect, photoelectrochemical reactions that convert solar energy into fuels (i.e., solar fuels) are being actively investigated [2, 3]. During photoelectrochemical solar fuel production, sunlight absorbed by a semiconductor generates photo-excited charge carriers (electrons and holes) that drive chemical reactions at a semiconductor/liquid electrolyte interface [3]. The most studied and developed solar fuel producing reaction is solar-driven water splitting to produce hydrogen fuel (H_2O + sunlight → H_2 + ½O_2). The successful implementation of solar hydrogen production into the energy landscape has the potential to secure a large portion of our future energy budget. However, to date, solar water splitting is either too inefficient and/or too expensive for commercialization. A major limitation is that much of the material development is hindered by a trial and error approach instead of a systematic one. An essential, missing ingredient needed for a systematic approach to solar-fuel generating material development is a molecular-level description of the semiconductor/electrolyte interface and changes at the interface induced by an applied voltage and/or incident light.

In this paper we present a general experimental means to gaining molecular-level information of the semiconductor/electrolyte interface. Our approach combines soft and hard X-ray ambient pressure photoelectron spectroscopy, AP-XPS and AP-HAXPES, respectively. Soft X-ray AP-XPS is inherently surface sensitive allowing the study of gas phase water adsorption on a semiconductor surface as well as the semiconductor in contact with a condensed liquid water or aqueous electrolyte film that is a few layers thick. Due to its increased information depth, hard X-ray AP-HAXPES allows the interrogation of the buried interface formed between a

semiconductor and a bulk-like, thin aqueous electrolyte layer. By combining these two techniques, the semiconductor/aqueous electrolyte interface can be studied as it is built-up in a step-wise fashion from its initial stages of formation to an interface closely resembling that found in a functioning water splitting device. The application of AP-photoelectron spectroscopy, AP-PES, (we will use AP-PES to designate generic photoelectron spectroscopy (i.e., with soft and/or hard X-rays) under ambient conditions) for studying solid/liquid interfaces is a relatively recent development [4, 5, 6, 7, 8]. Its implementation requires novel technical solutions to minimize the elastic and inelastic scattering of electrons by the liquid phase and the relatively high pressure of gas (the vapor pressure of water at 20 °C is 17.5 Torr). A major strength of using AP-PES to study semiconductor/electrolyte interfaces used in solar water splitting is that AP-PES can simultaneously measure both chemical composition and electrical potential. This allows the elemental and chemical specificity of PES to be correlated with accurately measured electrical potentials at the semiconductor surface as well as in the liquid phase. When AP-PES is used in conjunction with other complementary techniques (e.g., infrared spectroscopy, sum frequency generation spectroscopy, calorimetry, and general (photo)electrochemical techniques), the potential for a deeper understanding and discovering new phenomena about solid/liquid interfaces is great.

This paper is organized as follows. After presenting two examples of current challenges in solar fuels material development that AP-XPS and AP-HAXPES can directly address, we will provide a short description of soft and hard X-ray AP-XPS and AP-HAXPES focusing on their distinguishing and complementary characteristics. In this section, challenges in achieving monolayer sensitivity in solid/aqueous electrolyte studies will be discussed and combined AP-XPS and AP-HAXPES studies as a means to address this challenge will be proposed. This will be followed by an example of the application of combining AP-XPS and AP-HAXPES to study a

semiconductor/aqueous electrolyte interface currently used in water splitting devices. Specifically we will present data for the BiVO$_4$/aqueous potassium phosphate electrolyte interface and demonstrate how combining AP-XPS and AP-HAXPES provides molecular-level information about photo-induced changes at the BiVO$_4$/potassium phosphate electrolyte interface at open circuit potential.

Two current challenges in solar water splitting that can be addressed by AP-XPS and AP-HAXPES

During solar water splitting, charge is transferred across a solid/aqueous electrolyte interface to drive the oxidation and reduction half reactions that lead to the production of oxygen and hydrogen, at the anode and cathode respectively. The solid material that is in direct contact with the electrolyte can be the sunlight absorbing semiconductor, a protection layer that has been deposited on top of the absorbing semiconductor and/or a catalyst layer that is used to increase water splitting activity. Further, the solid/electrolyte interface may undergo a variety of changes that will depend on the specific conditions (e.g., applied potential, characteristics of the illumination source (wavelength and intensity), composition of the electrolyte and the materials used in the device). In turn, these changes will affect the photoelectrochemical activity. For example, specific ion adsorption can change the shape and the magnitude of the potential drop across the interface, catalyst layers deposited onto the semiconductor may passivate trap states and recombination centers, and the extreme pH values typically used for water splitting often lead to degradation of the semiconductor material over time. Understanding these processes on a molecular level could provide the basis for a rational approach to solar water splitting material development. Below we will briefly discuss two challenges in solar water splitting for which AP-XPS and AP-HAXPES can potentially provide valuable insight. These are: 1) understanding the role of catalyst layers in photoelectrochemical devices, and 2) correlating the chemical

4

composition of the semiconductor interface with band edge positions.

In-situ electrochemical investigation of catalyst layers

Since most semiconductors show low activity for water splitting, their surfaces are frequently modified by adding catalysts. Interestingly, some catalysts work well when combined with certain semiconductors but poorly with others [9]. The precise role that a catalyst plays in improving water splitting activity is currently not well understood. In some cases, the catalyst may act as a "true" catalyst by decreasing the activation barrier for charge transfer from the semiconductor to the catalyst/electrolyte interface [10]. In other cases the catalyst may simply passivate recombination centers which leads to an increase in water splitting efficiency but does not necessarily increase the charge transfer rate to the electrolyte. This was recently demonstrated in a study of cobalt phosphate catalysts deposited on $BiVO_4$ [11]. This study showed that the rate constant for charge transfer decreases with the addition of the catalyst but the overall water splitting activity increases due to a large reduction in the charge carrier recombination rate due to passivation of recombination centers by the catalyst [11].

Since the electronic and chemical characteristics of a catalyst depend on the specific conditions, *in-situ* or *operando* studies are necessary to decipher their precise role. For example, the concept of adaptive junctions at water splitting conditions has been proposed as an explanation for the success of some catalyst layers [9, 12]. In an adaptive junction, the catalyst layer is permeable to the electrolyte leading to mobile, charge compensating ions within the catalyst layer and no electrostatic potential drop within the catalyst layer or across the catalyst/electrolyte interface. As the catalyst drives the electrochemical reaction both the catalyst and the catalyst/electrolyte interface change and the work function of the catalyst "adapts" *in-situ*. Ni-Fe oxyhydroxide, currently among the most promising water oxidation catalysts, is an

example of an electrolyte permeable catalyst that has demonstrated such adaptive behavior. Using a dual-working-electrode experiment to independently monitor the potential and current in the semiconducting and catalyst layers, Boettcher et al. investigated adaptive behavior in a single crystal $TiO_2/NiOOH$, $Ni(OH)_2$ junction [12]. To make electrical contact to the catalyst layer, Au was deposited onto the $Ni(OH)_2$ layer. As the potential of the TiO_2 semiconductor was scanned an abrupt change in the potential of the $Ni(OH)_2$ catalyst layer was observed. Similar measurements with an IrO_x catalyst layer that does not display adaptive behavior showed a linear potential shift with changing semiconductor potential. While this work clearly demonstrates the potential of a dual-working-electrode experiment to monitor adaptive catalyst behavior, making good electrical contact to the catalyst via the Au layer is challenging and the deposition of the Au layer may, to some extent, modify the interface between the catalyst and the electrolyte. AP-PES techniques provide the possibility for *in-situ*, contactless, investigations of adaptive catalyst behavior. Shifts in core-level binding energies can be used to provide information about the electrostatic potential within the catalyst layer [13]. The distribution of the potential throughout the catalyst layer can be monitored with depth profiling measurements. Due to the chemical specificity of photoelectron spectroscopy, the changes in potential can be directly correlated with changes in the chemical composition of the catalyst. Such an approach was recently used to study Ni-Fe oxyhydroxide catalyst layers with AP-HAXPES where changes in the amount of hydroxylation could be correlated with binding energy shifts in the liquid electrolyte layer which served as a local work function probe [14].

Correlating interfacial chemistry and band edge positions

Band edge positions play a central role in electrochemical devices and proper band alignment is essential to the functioning of the device. In a tandem device an n-type semiconductor is used as the photoanode (where oxidation occurs) and a p-type semiconductor is

used as the photocathode (where reduction occurs). For the device to function effectively, the valence band maximum of the n-type material must be lower than the water oxidation (oxygen evolution) potential, so that holes are transferred to the electrolyte, and the conduction band minimum of the p-type semiconductor must be above the water reduction (hydrogen evolution) potential, to aid electron transfer. Solvation effects at the semiconductor/electrolyte interface can greatly affect the relative positions of the semiconductor band edges to the redox potentials of the electrolyte. For example, theoretical calculations of functionalized silicon surfaces have predicted that solvation effects induced by pure water can cause electronic state shifts of greater than 1.5 eV [15]. The magnitude of the solvation-induced shift depends on the nature of the interaction between the semiconductor surface and water; hydrophilic surfaces show larger shifts [15]. While theoretical calculations have demonstrated the ability to provide correlations between band edge positions and the chemical composition of the semiconductor/electrolyte interface, direct measurements of such correlations using experimental techniques are currently lacking [15, 16, 17 , 18].

XPS measurements allow the determination of energy levels relative to the Fermi level of the material under investigation. The binding energy of an electron is defined as the difference in energy between the level from which the photoelectron has been emitted and the Fermi level. In a semiconductor, the formation of a space-charge region at a junction between two materials or at the surface of the semiconductor itself causes the valence and conduction levels to bend upwards or downwards. A common assumption is that core-level binding energy shifts mirror the shifts in the valence band maximum induced by band bending. As a result, PES has been successfully used to correlate semiconductor band edge positions and band bending with the chemical composition of their surfaces [19, 20]. Such an approach has been recently used to study band alignment at the solid-solid interface formed between silicon and TiO_2 protection layers for

photoelectrochemical applications [21]. A standard experimental procedure for conducting these studies is to vacuum deposit a solid overlayer, layer-by-layer onto the substrate while simultaneously monitoring both valence and core-level spectra [22]. In this way the valence states and core level binding energy shifts can be monitored as the interface is formed to determine band alignment between the substrate and overlayer. A similar approach may be taken for semiconductor/liquid electrolyte interfaces.

By combining soft X-ray AP-XPS and AP-HAXPES experiments, semiconductor/electrolyte interfaces can be studied from their initial stages of formation to the formation of the interface between a semiconductor and a bulk-like electrolyte film. Given the potential for large solvation induced band edge position shifts, as discussed above, such studies promise to provide great insight into the chemical species responsible for large shifts in band edge positions. The approach used is illustrated in Figure 1. The semiconductor/electrolyte interface is "built-up" from left to right. The top row depicts experiments conducted in pure water vapor. Beginning from the left the surface is first measured in ultra-high vacuum conditions with soft X-ray XPS (1), then water vapor is introduced (2), at elevated pressures molecular water adsorbs and dissociates on the surface forming hydroxyl groups and a thin water film (3), in (4) we either illuminate the sample, apply a bias to the sample or both, so that the influence of illumination and applied bias can be studied, and in (5) AP-HAXPES is used to investigate the sample beneath a thin pure water film that is formed when the substrate is dipped into water and withdrawn (dip-and-pull) to form an extended meniscus [23]. In the bottom row, the same procedure is followed as in the top row except that before the introduction of water vapor a small amount of salt is deposited onto the sample (1). The water vapor pressure is then increased to the deliquescence point of the aqueous electrolyte solution. Once the deliquescence point is reached a thin aqueous electrolyte film is formed on the surface (3) [24]. In (4) we again subject the sample

to applied bias and/or illumination. In (5) the sample is dipped into an aqueous electrolyte solution and investigated with AP-HAXPES, again applying bias, illuminating or both. Such combined studies promise to provide great insight into the chemical composition of the semiconductor/electrolyte interface, how it changes as it is formed and how it correlates with band edge positions. External parameters such as applied bias and illumination can also be explored to determine their influence on the chemical composition of the interface as shown in Figure 1.

General aspects of studying semiconductor/aqueous electrolyte interfaces using AP-XPS and AP-HAXPES

For details about AP-PES with both soft and hard X-rays the reader is referred to the numerous existing reviews [25, 26, 27, 28, 29]. In this section we discuss the distinguishing and complementary features of AP-XPS and AP-HAXPES to demonstrate how their combination can be used to gain molecular-level insight into semiconductor/electrolyte interfaces used in solar water splitting devices focusing only on bulk-like electrolyte layers as opposed to the electrolyte film formation studies outlined above.

There are essentially two approaches to investigate solid/liquid interfaces for electrochemical applications with photoemission spectroscopy that differ by which side of the interface is used for X-ray incidence and electron detection. the solid or the liquid side [23, 30, 31]. Using supported membranes, such as graphene on a silicon nitride grid, or coated membranes, where the total thickness of the solid material is less than two to three times the mean free path of electrons, photoemission experiments can be conducted from the solid side of the solid/liquid interface (see Figure 2A) [30, 31]. When combined with a flow cell, this approach has the advantage that the liquid electrolyte can flow through the system thereby providing facile

mass transport in the liquid electrolyte. However, this technique is limited to the investigation of thin solid films (less than a few nm if performing AP-XPS, and approximately 30 nm if performing AP-HAXPES at photon energies of 4000 eV or more), since the photo-emitted electrons must travel through the solid to reach the analyzer. Performing these experiments without breaking the ultrathin films, which would result in electrolyte venting into the UHV system, has been demonstrated but is experimentally challenging. A second approach, using X-ray incidence and electron detection from the liquid side, (see Figure 2B), requires the formation of a thin liquid layer whose thickness does not exceed two to three times the mean free path of the electrons through the liquid electrolyte layer [23]. This has the advantage of being able to investigate a broader range of solid materials of arbitrary thickness but is currently limited by mass transport in the electrolyte layer since the liquid electrolyte layers are effectively static in the direction parallel to the solid surface. Since we focus on solar water splitting systems where practical semiconducting absorber layers are typically 100 nm or more (so that the semiconductor film thickness exceeds the absorption length of solar light) we will only discuss the approach using X-ray incidence and electron detection from the liquid side (see Figure 2B).

AP-XPS and AP-HAXPES are distinguished by their use of different photon energy ranges. Soft X-ray AP-XPS typically uses photon energies from less than 100 eV to approximately 2000 eV, whereas AP-HAXPES uses photon energies between 2500 eV and 10 keV. The higher photon energy of AP-HAXPES compared to AP-XPS increases the kinetic energy of a photo-emitted electron from a specific core-level. For example, the Bi 4f core-level in $BiVO_4$ has a binding energy of approximately 159.5 eV. Using a photon energy of 360 eV results in a kinetic energy of the photo-emitted electrons of about 200 eV, whereas using a photon energy of 4000 eV results in a photoelectron kinetic energy of about 3840 eV. This increase in photoelectron kinetic energy directly affects the information depth of the measurement. The

inelastic mean free path, λ, of photoelectrons through liquid water is slightly greater than 1 nm for 200 eV kinetic energy electrons and increases 10-fold to approximately 10 nm for 3840 eV kinetic energy electrons [32]. Assuming information depths of approximately 3 λ and that the thickness of one "layer" of water is about 3 Å [33], suggests that with 200 eV kinetic energy photoelectrons information depths are on the order of 3 nm, or 10 water monolayers, whereas with 3840 eV kinetic energy photoelectrons information depths are on the order of 30 nm, or 100 water monolayers. The differences in information depths for AP-HAXPES and AP-XPS have important consequences for studying semiconductor/electrolyte interfaces, these are discussed below.

Electrolyte concentration, minimum electrolyte layer thicknesses and monolayer sensitivity at the interface

Hydroxyl groups formed on a semiconductor surface are likely key intermediates for solar water splitting. In this section we consider the best approaches to detecting a monolayer of adsorbed hydroxyl groups on the surface of an oxide semiconductor or oxide containing catalyst that are formed via adsorption from aqueous hydroxide solutions. Although we only discuss hydroxyl groups in this section the results are applicable to other oxygen containing ions (e.g., phosphate, carbonate and sulfate ions) as long as the adsorbed state (ads) and the aqueous state (aq) have the same number of oxygen atoms. The challenge in detecting a monolayer of hydroxyl groups is a result of multiple oxygen containing components in the system: the oxide semiconductor or catalyst, the adsorbed hydroxyls, and the hydroxyls and the molecular water in the electrolyte solution. These multiple oxygen containing species give rise to complex O 1s spectra that may be difficult to de-convolute and quantify.

O 1s spectra taken in a AP-PES experiment of an oxide semiconductor in contact with an

aqueous hydroxide electrolyte can potentially contain peaks from gas phase water, $H_2O(g)$, liquid water in the electrolyte solution, $H_2O(l)$, hydroxyl groups in the electrolyte solution OH(aq), hydroxyl groups adsorbed on the semiconductor OH(ads) and oxygen in the semiconductor, $A_xB_yO_z(s)$. Previous AP-XPS studies of water adsorption on oxide surfaces have demonstrated that in most cases the O 1s peaks arising from $A_xB_yO_z(s)$, OH(ads), $H_2O(l)$ and $H_2O(g)$ have sufficient binding energy differences so as to be resolved in the O 1s spectra [55, 56, 57, 58, 59]. For example, AP-XPS studies of water adsorption on $TiO_2(110)$ measured O 1s binding energies for OH(ads) and molecular water that are about 1.3 eV and 3.0 eV higher than the O 1s binding energy of TiO_2 [59]. The gas phase water O 1s peak is located 5.0 eV higher in binding energy than the TiO_2 O 1s signal. These binding energy differences are all easily resolved using modern XPS equipment. O 1s peaks arising from OH(ads) and OH(aq), however, can have similar, nearly overlapping binding energies. For example, Winter et al. using a liquid jet technique to perform photoemission experiments of sodium hydroxide solutions [34] found that the O 1s binding energy difference between the OH(aq) and $H_2O(l)$ was approximately 2 eV. This is similar enough to the difference in O 1s binding energy between OH(ads) and $H_2O(l)$ observed in water adsorption experiments [55, 56, 57, 58, 59] that significant peak overlap between OH(ads) and OH(aq) can be expected. The question then becomes what are the relative intensities of the OH(ads) and OH(aq) O 1s peaks that can be expected? This relative intensity will depend on both the concentration of the electrolyte and the thickness of the electrolyte film.

If the thin electrolyte film used in "liquid-side" AP-PES experiments is to be representative of a bulk electrolyte solution, the electrolyte film should be thicker than the combined thickness of the Stern and diffuse layers of the electrical double layer. To quantify this thickness we set a minimum thickness of the electrolyte film to three times the Debye screening length (λ_D) of the electrolyte solution. At this distance, the potential applied to the semiconductor

surface is ~95% screened ($1/e^3$). Since λ_D depends on the ionic strength of the electrolyte solution, the minimum electrolyte film thickness will too. For aqueous solutions at 25 °C, $\lambda_D = 3.046{\times}10^{-10}/\sqrt{I}$ where $I = (1/2)\{\sum_i z_i^2 (m_i/m_o)\}$ is the ionic strength of the solution [35]. The sum in I is over all ions, i, in the solution, z_i^2 is the square of the ionic charge, m_i its concentration in molality and m_o is 1 mol/kg. We have calculated the minimum film thicknesses for a 1:1 electrolyte, such as KOH, for concentrations of 0.001 M, 0.01 M, 0.1 M and 1.0 M (see Table 1). These minimum electrolyte film thicknesses should provide the best possibility to detect a monolayer of OH(ads) on a flat semiconductor/electrolyte interface with bulk-like electrolyte films. Thicker electrolyte films will attenuate the OH(ads) signal more and have a higher contribution from OH(aq) in the O 1s spectra.

Using the calculated minimum electrolyte film thicknesses we can estimate the relative signal from OH(ads) and OH(aq) at the flat semiconductor/liquid interface. To do so, we have used the peak areas generated from model systems using the SESSA v1.3 software package [36]. Our model contains a 0.3 nm thick oxygen layer with $1{\times}10^{15}$ atoms/cm^2 to represent a monolayer of adsorbed OH (OH(ads)) (see Supporting Information for details). The O 1s signal from OH(ads) is attenuated by the electrolyte layer; the attenuation being predominantly caused by the water molecules in the electrolyte since the concentration of ions in solution is too low for them to contribute significantly to signal attenuation. To determine the amount of attenuation by the electrolyte layer we simulated the attenuation of a Si 2p signal as a function of water layer thickness, using photon energies of 3570 eV, 1570 eV and 300 eV giving photoelectron kinetic energies of approximately 3470 eV, 1470 eV and 200 eV respectively. The calculated attenuation factors are therefore representative of O 1s (BE ~ 530 eV) spectra taken with photon energies of 4000 eV, 2000 eV and 730 eV respectively. Table 1 reports the mean free path of the photoelectrons through the electrolyte layer found by fitting the Si 2p signal intensity as a

function of water overlayer thickness to a single exponential function (see S. I.). These values are in good agreement with those found in the literature [32]. The attenuation factors for OH(ads) are listed in Table 1 for each electrolyte film thickness and photon energy (kinetic energy of the photoelectrons). Based on the attenuation of the OH(ads) signal alone, it is apparent that to study solid/electrolyte interfaces photon energies of > 2000 eV are required unless the electrolyte concentration is high enough that very thin electrolyte films may be used.

Turning now to the expected ratio of the OH(ads) to OH(aq) integrated peak intensities, it is apparent from the values in Table 1 that the OH(ads) signal dominates over the OH(aq) signal if the ideal electrolyte film thickness can be used and the OH(ads) signal is not drastically attenuated. Further, for high concentrations of electrolytes (e.g., 0.1 M or 1.0 M, where very thin electrolyte films, 1 to 3 nm thick, can be used) it may be advantageous to use photon energies of approximately 2000 eV. Although the OH(ads) signal is slightly more attenuated using 2000 eV photons than with 4000 eV photons (0.52 compared to 0.72 for 0.1 M solutions, 3 nm thick films, and 0.83 compared to 0.88 for 1.0 M solutions, 1 nm thick films), the OH(ads) to OH(aq) ratio does not differ too drastically (39 versus 47 and 16 versus 16 for the 0.1 M and 1.0 M aqueous films, respectively). A potential advantage of 2000 eV energy photons is the higher photoionization cross-section (σ) at 2000 eV compared to 4000 eV. The O 1s photoionization cross-sections are listed at the bottom of Table 1 for each of the three photon energies considered. These values are taken from Trzhaskovskaya et al. [37, 38]. These values do not include dipole, non-dipole or second order contributions since the magnitude of their contribution to the cross-section will depend on the specific experimental geometry. The O 1s photoionization cross-section for 2000 eV photons is approximately 8 times higher than for 4000 eV photons which will lead to significantly higher signal intensities and shorter integration times.

So far, we have only discussed trends for ideally thin electrolyte films on flat surfaces for a given

14

electrolyte concentration. More generally the electrolyte films used for liquid side AP-HAXPES experiments are not of controlled thicknesses. To consider the effects of electrolyte films that are thicker than the ideal thickness, the OH(ads)/OH(aq) ratio listed in Table 1 can simply be scaled by the electrolyte concentration for a specific film thickness and photon energy. The attenuation factors remain approximately the same for a given electrolyte film thickness since the attenuation is mainly due to the water molecules in the solution. For example, an O 1s spectrum of a 30 nm thick film of a 1.0 M KOH electrolyte solution taken with 4000 eV photon energy will have an OH(ads)/OH(aq) value of 0.072, since the OH(aq) signal increases 1000-fold when increasing the KOH concentration from 0.001 to 1.0. The OH(ads) attenuation factor is 0.038. This indicates that for some combinations of high electrolyte concentrations and thick electrolyte films (e.g., 0.1 M and 30 nm thick, or 1.0 M and 10 nm thick) the signals from OH(ads) and OH(aq) are similar in intensity and care must be taken when de-convoluting the O 1s spectra. For 1.0 M, 30 nm thick electrolyte films the OH(aq) signal will be much stronger than the OH(ads) signal by about a factor of 14. This emphasizes the importance of being able to generate thin electrolyte films of a specified thickness. We expect this to be of key importance for the future, broader application of AP-HAXPES to study semiconductor/electrolyte interfaces. In addition, by being able to generate arbitrarily thin electrolyte films, soft X-ray AP-XPS can be used where higher photoionization cross-sections can lead to shorter integration times, as long as high electrolyte concentration solutions are studied so that the thin electrolyte film has bulk-like properties or can be used to efficiently model bulk configurations. Lastly, as previously suggested and shown in Figure 1, if arbitrarily thin aqueous electrolyte films cannot be easily generated, a potential means of gaining detailed chemical information about semiconductor/aqueous electrolyte interfaces is to conduct gas phase water adsorption studies. In particular, we envision performing combined studies of pure water adsorption and the deliquescence of a previously deposited solid electrolyte generate

15

thin aqueous electrolyte films (that may not be bulk-like). Such vapor phase studies should provide a reasonable, qualitative approximation of the chemical species present when the solid is in contact with a bulk-like electrolyte. The connection between the gas phase AP-XPS studies and AP-HAXPES studies at semiconductor/bulk-like aqueous electrolyte interfaces can be strengthened by building the electrolyte film in a step-wise manner (see Figure 1), a method analogous to what has long been used in UHV conditions to understand solid/solid interfaces [39, 40].

Photo-induced changes at the BiVO$_4$/potassium phosphate aqueous electrolyte interface at open circuit potential studied with AP-XPS and AP-HAXPES

In this section we provide an example of combining AP-XPS and AP-HAXPES measurements to understand photo-induced changes at the interface formed between a complex semiconducting oxide and an aqueous electrolyte solution. The approach taken is similar to that as outlined in Figure 1. We first studied gas phase adsorption of water on a single crystal of BiVO$_4$ and then the interface formed between a thin BiVO$_4$ film and a 0.1 M potassium phosphate (KPi) aqueous electrolyte solution. The AP-XPS experiments were carried out on a BiVO$_4$(010) single crystal surface at beamline 11.0.2 of the Advanced Light Source (ALS) at Lawrence Berkeley National Laboratory. The AP-HAXPES measurements were performed instead at beamline 9.3.1 of the ALS. For the AP-HAXPES experiments a 100 nm thick BiVO$_4$ film deposited onto an FTO/glass substrate with spray pyrolysis was used [41], which is similar to that used in a practical water splitting device.

AP-XPS of water adsorption on BiVO$_4$(010).

The adsorption of pure water onto the (010) surface of 1% Mo-doped BiVO$_4$ single crystals was studied using AP-XPS. 1% doping with Mo is sufficient to make the crystals

16

conductive enough to perform PES. Single crystals of $BiVO_4$ are rare and experiments with them are limited. The first synthetic single crystals of $BiVO_4$ were made by Sleight et al. in 1979 [42] and to date most experiments with $BiVO_4$ single crystals have focused on its intrinsic conduction properties [43, 44, 45]. To our knowledge, this is the first experimental study of water adsorption on the $BiVO_4(010)$ surface.

Theoretical studies have investigated the bulk and surface properties of $BiVO_4$, and its doping with Mo [46, 47, 48, 49, 50, 51, 52, 53, 54]. The (010) surface is calculated to have the lowest energy for the monoclinic scheelite phase [49]. Calculations of water adsorption on both the (100) and (110) surfaces of $BiVO_4$ have been previously performed [51, 52, 53, 54]. These calculations indicate that water does not dissociate (i.e., it adsorbs molecularly), whether the surface is doped or undoped. Mo doping at the (010) surface (in Bi sites [50]) increases the adsorption energy of water, and the preferred adsorption site is on top of the surface Bi atoms for both doped and undoped $BiVO_4$. We note that AP-XPS results for water adsorption on numerous single crystalline oxide surfaces, including, $MgO(100)$ [55, 56], $Fe_2O_3(0001)$ [57], $Fe_3O_4(001)$ [58] and $TiO_2(110)$ [59] have indicated significant surface hydroxylation (i.e., water dissociation) in the sub-1 Torr water vapor pressure range (see reference [25] for a summary of water adsorption on oxide surfaces studied with AP-XPS).

The 1%-Mo doped $BiVO_4$ crystals used in our experiments were grown at the Leibniz-Institut für Kristallzüchtung in Berlin, Germany.Prior to introduction into the vacuum chamber, the single crystals were cleaved on the lab bench. After introduction into the vacuum system, the crystal was heated to about 300 °C in approximately 1 Torr of $O_2(g)$ to remove most of the surface carbon. The C to surface Bi, or surface V, ratio is estimated to be 0.08 for the starting surface at room temperature in UHV. Despite the carbon on the surface, a reasonably sharp LEED pattern could be obtained (Figure 3). The observed square LEED pattern is consistent with

the (010) surface of $BiVO_4$.

O 1s spectra collected at 4 x 10^{-8} Torr and 0.62 Torr water vapor pressure using AP-XPS are shown in Figure 4. At 4 x 10^{-8} Torr the $BiVO_4$(010) surface is free of hydroxyl groups. At 0.62 Torr there is extensive hydroxylation of the surface in addition to molecularly adsorbed water consistent with previous AP-XPS studies of water adsorption on oxide surfaces [25, 55, 56, 57, 58, 59] but in contradiction to the theoretical calculations for water adsorption on $BiVO_4$(010) [51, 52, 53, 54]. V 2p spectra collected at 4 x 10^{-8} Torr and 0.62 Torr water vapor pressure using AP-XPS are also shown in Figure 4. At 4 x 10^{-8} Torr the $BiVO_4$(010) surface is composed of mostly V^{5+} but once hydroxylated a significant amount of V^{4+} is observed in the surface region. These measurements indicate that the $BiVO_4$ surface in contact with the potassium phosphate electrolyte (pH = 7.0) presented below likely contains significant amount of hydroxyl species as well as reduced vanadium (V^{4+}) in the surface region.

AP-HAXPES of BiVO₄/potassium phosphate aqueous electrolyte interface under illumination with solar light

We have used AP-HAXPES with an excitation energy of 4000 eV to study the chemical properties of the interface formed between a $BiVO_4$ thin film and a 0.1 M KPi aqueous electrolyte and changes induced by illumination with solar light in an electrochemical cell open circuit potential (OCP). Our results are summarized in Figure 5.

The initial O 1s spectrum taken in the dark (Figure 5, bottom, left) shows peaks that can be attributed to the $BiVO_4$ film (lattice oxygen, O^{2-}), the phosphate ions in solution, and water in the liquid and gas phases. The ratio of the H_2O(l) to $BiVO_4$ O 1s peak areas can be used to estimate the thickness of the electrolyte film [32, 60]. The peak area ratio is 14.2 and indicates that the electrolyte film thickness is approximately 21 nm thick. This film is thick enough to be

considered a bulk-like electrolyte film since it far exceeds the thickness required for 3 Debye lengths (see Table 1 for an estimate of this thickness for 1:1 electrolytes). Considering the values presented for signal intensity ratios between adsorbed ions and aqueous ions in S. I. Table 1, (OH(ads)/OH(aq) = 2.37 for hv = 4000 eV, 20 nm thick electrolyte film) the peak located at 530.9 eV could be due to phosphate ions in solution, adsorbed phosphate ions or even adsorbed hydroxyl groups since gas phase water adsorption experiments have indicated that hydroxyl groups readily form on the $BiVO_4$ surface (see above section and note that at pH = 7 (the pH of the KPi buffer solution the OH(aq) is at far too low of a concentration to be detected). Upon illumination with a 100W Xe lamp solar simulator (Asahi HAL-C100, 1 sun, 400-1100 nm) two noticeable changes occur in the O 1s spectrum. First the $BiVO_4$ O 1s signal disappears. This is most likely a consequence of an increase in the aqueous electrolyte layer thickness due to a change in the wetting properties of the $BiVO_4$ film resulting from a chemical modification to the $BiVO_4$ film surface. Using the rough estimate for our detection limit of ~0.25 of the initial $BiVO_4$ O 1s signal in the dark (Figure 5, left, bottom) we can approximate that the liquid electrolyte film for the O 1s spectrum with the solar simulator on is at least 33 nm thick. This increase in electrolyte film thickness would further attenuate any signal due to adsorbed ions on the $BiVO_4$ film surface. The second noticeable change in the spectrum when turning the solar simulator on is an increase in the ratio of integrated intensity of the peak due to phosphate ions, either adsorbed or in solution, and adsorbed hydroxyl groups to the liquid water peak. This ratio increases from 0.16 to 0.36, i.e., a factor of 2.26. Since the signal from adsorbed species should be further attenuated by the increase in the electrolyte layer thickness upon illumination, the observed increase in the signal ratio is likely due to migration of phosphate ions away from the $BiVO_4$/electrolyte interface towards the electrolyte/vapor interface. For adsorbed phosphate ions or adsorbed hydroxyl groups to be responsible for the observed increase in signal ratio their

surface concentration would have to increase by at least a factor of 7. That the peak located at 530.89 eV is due to aqueous phase ions, rather than adsorbed species, is further supported by the observation that when returning to dark conditions the ratio of this peak to the liquid water peak decreases back to 0.17, nearly equal to the ratio for the spectrum before turning on the solar simulator, but the $BiVO_4$ O 1s signal is still not visible (i.e., the electrolyte film remains thicker than 33 nm thick).

The right hand panel in Figure 5 shows Bi 4f spectra taken for the same conditions as those for the O 1s shown in the left hand panel. When turning the solar simulator on we also observe changes in the Bi 4f spectrum. First the Bi 4f signal attenuates, which is consistent with a thicker electrolyte film attenuating the signal. This attenuation remains upon returning to dark conditions consistent with the explanations for the changes in the O 1s spectra discussed above. Further, upon illumination with the solar simulator we observe a broadening of the Bi 4f spectrum to higher binding energy. The binding energy of the Bi $4f_{7/2}$ level prior to illumination with the solar simulator and with the thin potassium phosphate electrolyte film is 158.7 eV (Figure 5, right, bottom). Keeping the same shape for the peak located at 158.7 eV and adding a peak to the Bi 4f spectrum to capture the broadening induced by illumination with the solar simulator gives a Bi $4f_{7/2}$ peak at a binding energy of 159.8 eV. The binding energy difference (1.1 eV) between the two Bi 4f peaks is too high to be a result of band flattening since the maximum amount of initial band bending is estimated to be approximately 300 meV [61]. A binding energy of 159.8 eV is, however, consistent with the formation of bismuth phosphate ($BiPO_4$) [62, 63, 64]. Interestingly, upon returning to dark conditions the broadening of the Bi 4f peak disappears, indicating reversible chemistry at the Bi centers induced by solar light illumination.

Model for changes at the $BiVO_4$/potassium phosphate electrolyte interface upon illumination with

solar light

Putting together the behavior of the O 1s and Bi 4f spectra upon solar light illumination and adding the information garnered from the AP-XPS experiments for water adsorption on $BiVO_4$ (010) allows us to propose the following tentative model to rationalize the changes observed at the $BiVO_4$/KPi electrolyte interface upon illumination at open circuit potential. First, since water adsorption studies on single crystals with soft X-rays indicate the presence of hydroxyl groups and reduced vanadium (V^{4+}) at the surface, the $BiVO_4$ film likely has hydroxyl groups and reduced vanadium (V^{4+}) centers in the near-surface region when in contact with the potassium phosphate electrolyte. Upon illumination, H^+ leaves the surface and is buffered by the potassium phosphate solution (as indicated by the increase in the relative amount of $H_2PO_4^-$ to HPO_4^{2-} measured by IR of the solution under illumination, see S.I. Figure 3). In addition, phosphate groups adsorb on the surface, forming bismuth phosphate. The combination of H^+ loss and phosphate adsorption charges the $BiVO_4$ surface more negatively as confirmed by the decrease of the OCP value of about 30 meV passing from dark (+175 mV) to light conditions (+144 mV) (the potentials reported here are measured against the $Ag/AgCl/Cl^-$(sat.) reference electrode). The more negatively charged surface repels the phosphate ions away from the $BiVO_4$/KPi electrolyte interface towards the KPi electrolyte/vapor interface. Upon returning to the dark conditions the reverse process occurs, i.e. the surface is less negatively charged and phosphate ions are less repelled from the $BiVO_4$/KPi electrolyte interface. We are currently conducting further studies in order to verify this tentative explanation. The studies to date, however, provide a simple example of how AP-XPS and AP-HAXPES studies can be combined to provide molecular-level detail of processes at the surfaces of water oxidation photoanodes.

Summary and Future Outlook

AP-XPS using soft X-rays is a well-established technique for studying adsorption of gas phase species onto solid surfaces. In general, the application of AP-PES techniques to study photoelectrochemical systems that use aqueous electrolytes is a recent development. This has been aided by the recent development of AP-PES using hard X-rays, i.e., AP-HAXPES that allows for the direct interrogation of solid/electrolyte interfaces in the presence of a bulk-like electrolyte. However, as described in this paper, potential challenges arise due to core-level peak overlap and limited peak intensities in AP-HAXPES measurements. A potential means to gain more detailed information is to combine the AP-HAXPES measurements with soft X-ray AP-XPS in the presence of pure water vapor. One then has to assume that the vapor phase studies provide a reasonable, qualitative approximation of the chemical species present when the solid is in contact with a bulk-like electrolyte. This connection can be strengthened by conducting studies where thin electrolyte films are built up in a step-wise manner; a method analogous to what has long been used in UHV conditions to understand solid/solid interfaces.

Future developments in the field will likely involve other advanced AP-spectroscopic techniques. In particular, gaining detailed information about the valence band of photoanode materials during photoelectrochemical reaction is particularly important for electrochemical systems since charge transfer processes are at the heart of their function. Ideally, band mapping using angle resolved photoemission spectroscopy (ARPES) in ambient conditions would be applied to fully understand the electronic states in these complex systems. To date, ARPES in ambient conditions has not been broadly applied although it has been demonstrated for solid/gas interfaces [65]. For solid/liquid interfaces such studies will likely be complicated by contributions from both the liquid and gas phase to the spectra. A potential means to enhance specific features in the valence band and therefore de-convolute the valence band into a projected density of states, is to perform resonant photoemission [66].

Advanced ambient pressure photoelectron spectroscopic techniques using X-ray standing waves (XSW) have already been applied to gain structural information about solid/electrolyte interfaces [24]. We expect the XSW technique to be applied quite extensively in the future to gain *operando* information about changes in the distribution of ions in the double layer induced by light illumination and applied voltage. In particular, such studies would be extremely valuable for understanding in greater detail the behavior of phosphate ions at the $BiVO_4$/KPi interface under illumination by sunlight as presented here.

References

[1] N. S. Lewis, D. G. Nocera, *Proceedings of the National Academy of Sciences USA* 103 (2006) 15729.

[2] K. Sivula, R. van de Krol, *Nature Reviews: Materials* 1 (2016) 15010.

[3] R. van de Krol, M. Grätzel in: R. van de Krol, M. Grätzel (Eds.), Photoelectrochemical Hydrogen Production, Springer, New York, 2012.

[4] M. F. Lichterman, S. Hu, M. H. Richter, E. J. Crumlin, S. Axnanda, M. Favaro, W. Drisdell, Z. Hussain, T. Mayer, B. S. Brunschwig, N. S. Lewis, Z. Liu, H.- J. Lewerenz *Energy Environ. Sci.* **8**, 2409 (2015).

[5] L. Trotochaud, A. R. Head, O. Karslioğlu, L. Kyhl, H. Bluhm J. Phys.-Condens. Mat. **29**, 053002 (2017).

[6] M. Favaro, W. S. Drisdell, M. A. Marcus, J. M. Gregoire, E. J. Crumlin, J. A. Haber, J. Yuno *ACS Catal.* **7**, 1248 (2017).

[7] M. Favaro, B. Jeong, P. N. Ross, J. Yano, Z. Hussain, Z. Liu, E. J. Crumlin *Nat. Commun.* **7**, 12695 (2016).

[8] M. Favaro, C. Valero-Vidal, J. Eichhorn, F. M. Toma, P. N. Ross, J. Yano, Z. Liu, E. J. Crumlin *J. Mater. Chem. A* (2017) DOI: 10.1039/c7ta0409e.

[9] M. R. Nellist, F. A. L. Laskowski, F. Lin, T. J. Mills, S. W. Boettcher *Acc. Chem. Res.* **49**, 733 (2016).

[10] S. J. A. Moniz, S. A. Shevlin, D. J. Martin, Z.-X. Guo, J. Tang *Energy Environ. Sci.* 8 (2015) 731.

[11] C. Zachäus, F. F. Abdi, L. M. Peter, R. van de Krol (*submitted*).

[12] F. Lin, S. W. Boettcher *Nat. Mater.* 13 (2014) 81.

[13] M. Favaro, B. Jeong, P. N. Ross, J. Yano, Z. Hussain, Z. Liu, E. J. Crumlin *Nat. Comm.* **7**, 12695 (2016).

[14] H. Ali-Löytty, M. W. Louie, M. R. Singh, L. Li, H. G. Sanchez Casalongue, H. Ogasawara, E. J. Crumlin, Z. Liu, A. T. Bell, A. Nilsson, D. Friebel *J. Phys. Chem. C,* **120**, 2247 (2016).

[15] T. A. Pham, D. Lee, E. Schwegler, G. Galli *J. Am. Chem. Soc.* **136**, 17071 (2014).

[16] Y. Ping, R. Sundararaman, W. A. Goddard III *Phys. Chem. Chem. Phys.* **17**, 30499 (2015).

[17] J. Cheng, M. Sprik *Phys. Chem. Chem. Phys.* **14**, 11245 (2012).

[18] N. Kharche, J. T. Muckerman, M. S. Hybertsen *Phys. Rev. Lett.* **113**, 176802 (2014).

[19] D. C. Gleason-Roher, B. S. Brunschwig, N. S. Lewis *J. Phys. Chem. C* **117** 18301, (2013).

[20] A. Klein, T. Mayer, A. Thissen, W. Jägermann in: R. Schäfer, P. C. Schmidt (eds.), Methods in Physical Chemistry, Wiley-VCH Verlag GmbH, 2012.

[21] S. Hu, M. H. Richter, M. F. Lichterman, J. Beardslee, T. Mayer, B. S. Brunschwig, N. S. Lewis *J. Phys. Chem. C* **120** 3117, (2016).

[22] A. D. Katnani, G. Margaritondo *Phys. Rev. B* **28**, 1944 (1983).

[23] S. Axnanda, E. J. Crumlin, B. Mao, S. Rani, R. Chang, P. G. Karlsson, M. O. M. Edwards, M. Lundqvist, R. Moberg, P. Ross, Z. Hussain, Z. Liu *Sci. Rep.* 5 (2015) 9788.

[24] S. Nemšak, A. Shavorskiy, O. Karslioglu, I. Zegkinoglou, A. Rattanachata, C. S. Conlon, A. Keqi, P. K. Greene, E. C. Burks, F. Salmassi, E. M. Gullikson, S.-H. Yang, K. Liu, H. Bluhm, C. S. Fadley *Nat. Commun.* 5 (2014) 5441.

[25] D. E. Starr, Z. Liu, M. Hävecker, A. Knop-Gericke, H. Bluhm *Chem. Soc. Rev.,* 42 (2013) 5833.

[26] M. Salmeron, R. Schlögl, *Surf. Sci. Rep.,* 63 (2008) 169.

[27] H. Bluhm, *J. Electron Spectrosc. Relat. Phenom.,* 177 (2010) 71.

[28] Z. Liu, H. Bluhm in: J. C. Woicik (ed.), Hard X.ray Photoelectron Spectroscopy (HAXPES), Springer, Cham, 2016.

[29] K. A. Stoerzinger, W. T. Hong, E. J. Crumlin, H. Bluhm, Y. Shao-Horn, *Acc. Chem. Res.*, 48 (2015) 2976.

[30] J. J. Velasco-Vélez, V. Pfeifer, M. Hävecker, R. Wang, A. Centeno, A. Zurutuza, G. Algara-Siller, E. Stotz, K. Skorupska, D. Teschner, P. Kube, P. Braeuninger-Weimer, S. Hofmann, R. Schlögl, A. Knop-Gericke *Rev. Sci. Instrum.* 87 (2016) 053121.

[31] J. J. Velasco-Vélez, V. Pfeifer, M. Hävecker, R. S. Weatherup, R. Arrigo, C.-H. Chuang, E. Stotz, G. Weinberg, M. Salmeron, R. Schlögl, A. Knop-Gericke *Angew. Chem. Int. Ed.* 54 (2015) 14554.

[32] D. Emfietzoglou, H. Nikjoo *Rad. Res.*, 167 (2007) 110.

[33] G. E. Ewing *Chem. Rev.,* 106 (2006) 1511.

[34] B. Winter, M. Faubel, R. Vácha, P. Jungwirth *Chem. Phys. Lett.* 474 (2009) 241.

[35] C. H. Hamann, A. Hamnett, W. Vielstich, Electrochemistry, 2 ed., Wiley-VCH, Weinheim, 2007.

[36] Werner, W. S. M.; Smekal, W.; Powell, C. J. *NIST Database for the Simulation of Electron Spectra for Surface Analysis, Version 1.3*, National Institute of Standards and Technology: Gaithersburg, MD, USA, 2011.

[37] M. B. Trzhaskovskaya, V. I. Nefedov, V. G. Yarzhemsky *Atomic Data and Nuclear Data Tables* 77 (2001) 97.

[38] M. B. Trzhaskovskaya, V. K. Nikulin, V. I. Nefedov, V. G. Yarzhemsky *Atomic Data and Nuclear Data Tables* 92 (2006) 245.

[39] A. D. Katnani, G. Margaritondo *Phys. Rev. B* **28**, 1944 (1983).

[40] P. H. Mahowald, R. S. List, W. E. Spicer, J. Woicik, P. Pianetta *J. Vac. Sci. Technol. B* **3**, 1252 (1985).

[41] F. F. Abdi, R. van de Krol *J Phys. Chem. C* 116 (2012) 9398.

[42] A. W. Sleight, H. Y. Chen, A. Ferretti, D. E. Cox *Mater. Res. Bull.* 14 (1979) 1571.

[43] L. Hoffart, U. Heider, L. Joerissen, R. A. Huggins, W. Witschel, R. Jooss, A. Lantz *Ionics* 2 (1996) 34.

[44] A. J. E. Rettie, W. D. Chemelewski, J. Lindemuth, J. S. McCloy, L. G. Marshall, J. Zhou, D. Emin, C. B. Mullins*Appl. Phys. Lett.* 106 (2015) 022106.

[45] A. J. E. Rettie, H. C. Lee, L. G. Marshall, J.-F. Lin, C. Capan, J. Lindemuth, J. S. McCloy, J. Zhou, A. J. Bard, C. B. Mullins *J. Am. Chem. Soc.* 135 (2013) 11389.

[46] Z. Zhao, Z. Li, Z. Zou *Phys. Chem. Chem. Phys.* 13 (2011) 4746.

[47] W. -J. Yin, S.-H. Wei, M. M. Al-Jassim, J. Turner, Y. Yan *Phys. Rev. B* 83 (2011) 155102.

[48] K. E. Kweon, G. S. Hwang *Phys. Rev. B* 86 (2012) 165209.

[49] Z. Zhao, Z. Li, Z. Zou *RSC Advances* 1 (2011) 874.

[50] K. Ding, B. Chen, Z. Fang, Y. Zhang, Z. Chen *Phys. Chem. Chem. Phys.* 16 (2014) 13465.

[51] M. Oshikiri, M. Boero, A. Matsushita, J. Ye *J. Electroceram.* 22 (2009) 114.

[52] M. Oshikiri, M. Boero *J. Phys. Chem. B* 110 (2006) 9188.

[53] J. Yang, D. Wang, X. Zhou, C. Li *Chem. Eur. J.* 19 (2013) 1320.

[54] R. Crespo-Otero, A. Walsh *J. Phys. Chem. Lett.* 6 (2015) 2379.

[55] J. T. Newberg, D. E. Starr, S. Yamamoto, S. Kaya, T. Kendelewicz, E. R. Mysak, S. Porsgaard, M. B. Salmeron, G. E. Brown, A. Nilsson, H. Bluhm *Surf. Sci.* 605 (2011) 89.

[56] J. T. Newberg, D. E. Starr, S. Yamamoto, S. Kaya, T. Kendelewicz, E. R. Mysak, S. Posgaard, M. B. Salmeron, G. E. Brown Jr., A. Nilsson, H. Bluhm *J. Phys. Chem. C* 115 (2011) 12864.

[57] S. Yamamoto, T. Kendelewicz, J. T. Newberg, G. Ketteler, D. E. Starr, E. R. Mysak, K. J. Andersson, H. Ogasawara, H. Bluhm, M. Salmeron, G. E. Brown Jr., A. Nilsson *J. Phys. Chem. C* 114 (2010) 2256.

[58] T. Kendelewicz, S. Kaya, J. T. Newberg, H. Bluhm, N. Mulakaluri, W. Moritz, M. Scheffler, A. Nilsson, R. Pentcheva, G. E. Brown, Jr. *J. Chem. Phys. C* 117 (2013) 2719.

[59] G. Ketteler, S. Yamamoto, H. Bluhm, K. Andersson, D. E. Starr, D. F. Ogletree, H. Ogasawara, A. Nilsson, M. Salmeron, *J. Phys. Chem. C* 111 (2007) 8278.

[60] S. Hofmann, Auger- and X-ray Photoelectron Spectroscopy in Materials Science, A User-Oriented Guide, Springer, Heidelberg, 2013.

[61] F. F. Abdi, L. han, A. H. M. Smets, M. Zeman, B. Dam, R. van de Krol *Nat. Commun.* 4:2195 doi: 10.1038/ncomms3195 (2013).

[62] Y. Zhang, H. Fan, M. Li, H. Tian *Dalton Trans.* **42**, 13172 (2013).

[63] M. H. Fulekar, A. Singh, D. P. Dutta, M. Roy, A. Ballal, A. K. Tyagi *RSC Adv.* **4**, 10097 (2014).

[64] M. Yang, N. K. Shrestha, R. Hahn, P. Schmuki *Electrochem. Solid St.* **13**, C5 (2010).

[65] M. E. Grass, P. G. Karlsson, F. Akoy, M. Lundqvist, B. Wannberg, B. S. Mun, Z. Hussain, Z. Liu *Rev. Sci. Instrum.* **81**, 053106 (2010).

[66] E. I. Solomon, L. Basumallick, P. Chen, P. Kennepohl *Coordin. Chem. Rev.* **249**, 229 (2005).
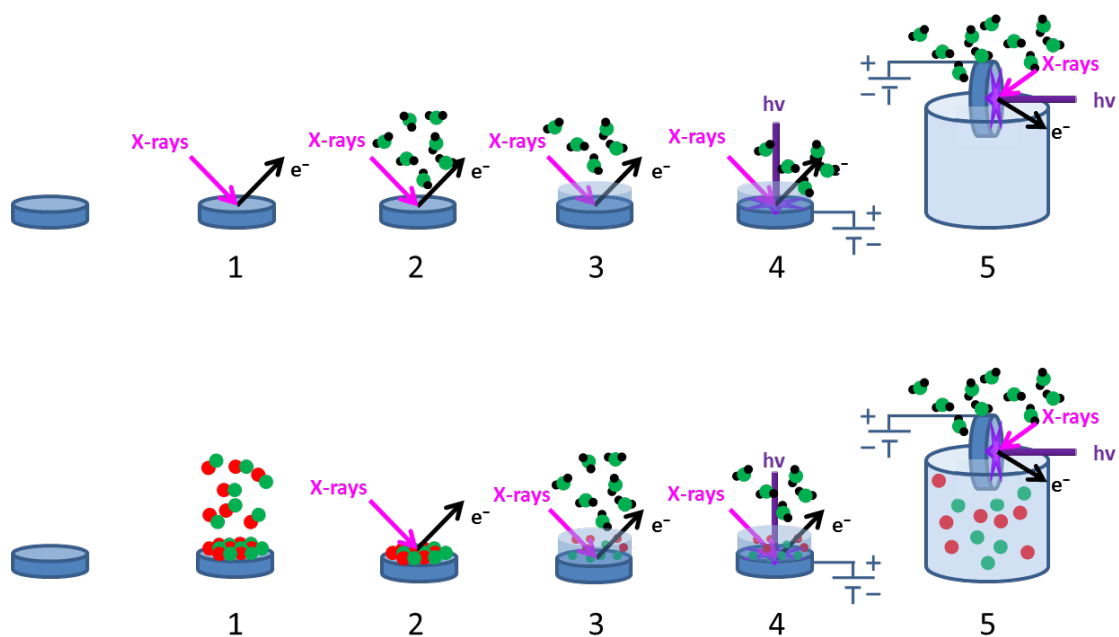
Figure 1: Combining soft and hard X-ray ambient pressure photoelectron spectroscopy for a molecular-level understanding of solid/electrolyte interfaces. The approach is similar to that used to study solid/solid interfaces; the interface is studied with increasing thickness of the overlayer, in this case the electrolyte. The electrolyte layer increases in thickness from left to right in the figure as the water vapor pressure is increased at constant temperature (i.e., the relative humidity increases). Soft X-ray AP-XPS is used from steps 1 to 4 while hard X-ray AP-HAXPES is used in 5. See text for details.
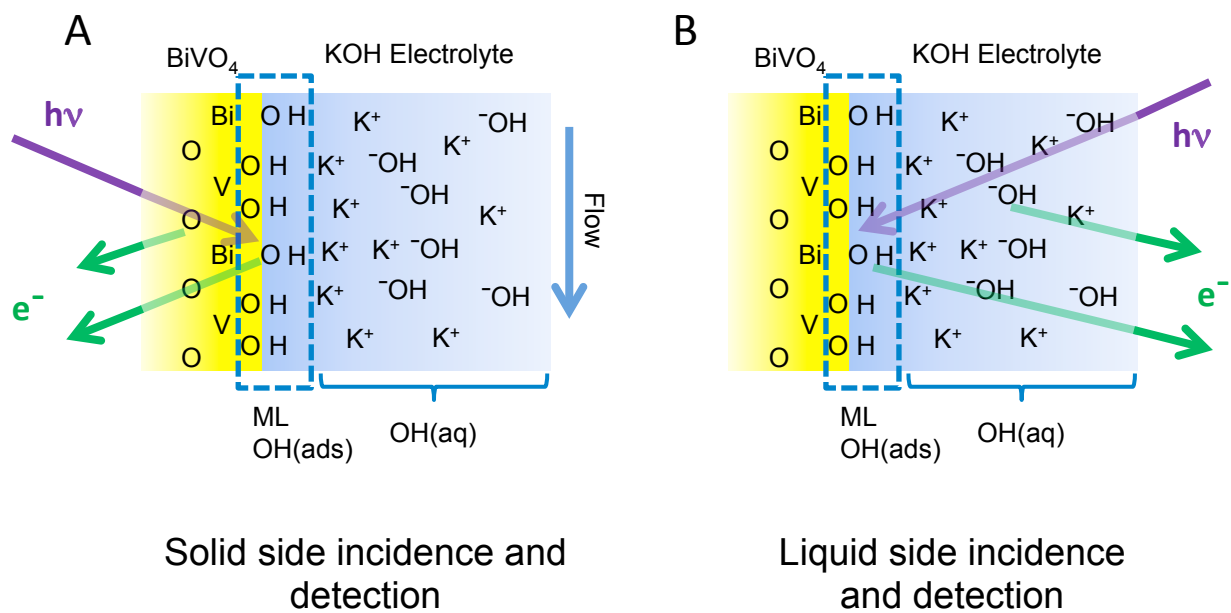
Figure 2: Two general approaches to studying solid/electrolyte interfaces for photoelectrochemical applications using AP-PES: A) solid-side incidence and detection, and B) liquid side incidence and detection.

Table 1: Minimum thickness required for a bulk-like electrolyte film (defined as three Debye lengths) for various concentrations of aqueous KOH electrolyte. Attenuation of the O 1s signal from a monolayer of OH(ads) and ratio of O 1s signals from the adsorbed monolayer of OH to the ⁻OH in solution, OH(ads) to OH(aq), for three different photon energies at the minimum electrolyte layer thickness for a specific concentration of aqueous KOH solution. For $h\nu$ = 730 eV only the two thinnest electrolyte layers are listed.

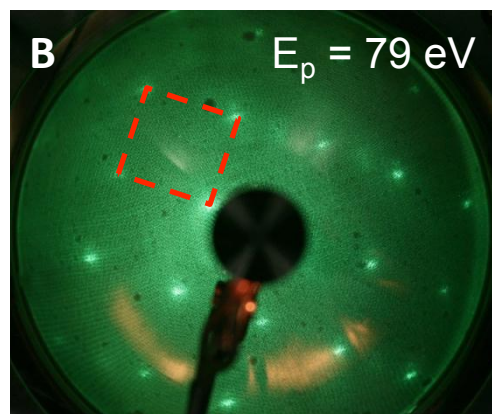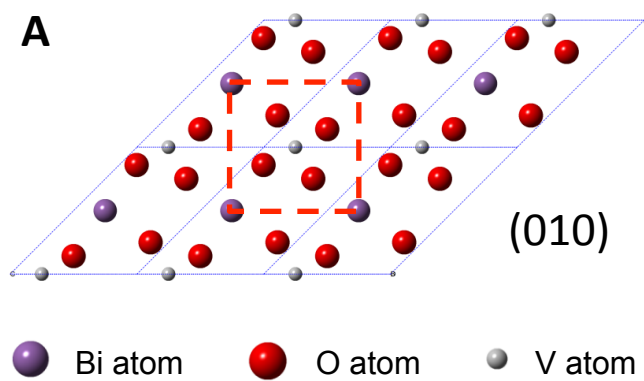| KOH [M]	Min. Electrolyte Layer Thickness [nm]	OH(ads) atten. factor	OH(ads)/ OH(aq)	OH(ads) atten. factor	OH(ads)/ OH(aq)	OH(ads) atten. factor	OH(ads)/ OH(aq)
0.001	30	----	----	7.7×10^{-4}	2.9	0.038	72
0.01	10	----	----	0.097	41	0.33	91
0.1	3	0.041	7.6	0.52	39	0.72	47
1.0	1	0.36	9.8	0.83	16	0.88	16
		$h\nu$ = 730eV, KE = 200eV λ = 0.97 nm, σ = 221		$h\nu$ = 2000eV, KE = 1470eV λ = 4.5 nm, σ = 15.7		$h\nu$ = 4000eV, KE = 3470eV λ = 9.2 nm, σ = 1.97	

Figure 3: A) The (010) surface of $BiVO_4$ with the surface unit cell shown by the red dashed lines. The LEED pattern from the prepared (010) surface of $BiVO_4$. The expected square pattern is highlighted by the dashed red lines.
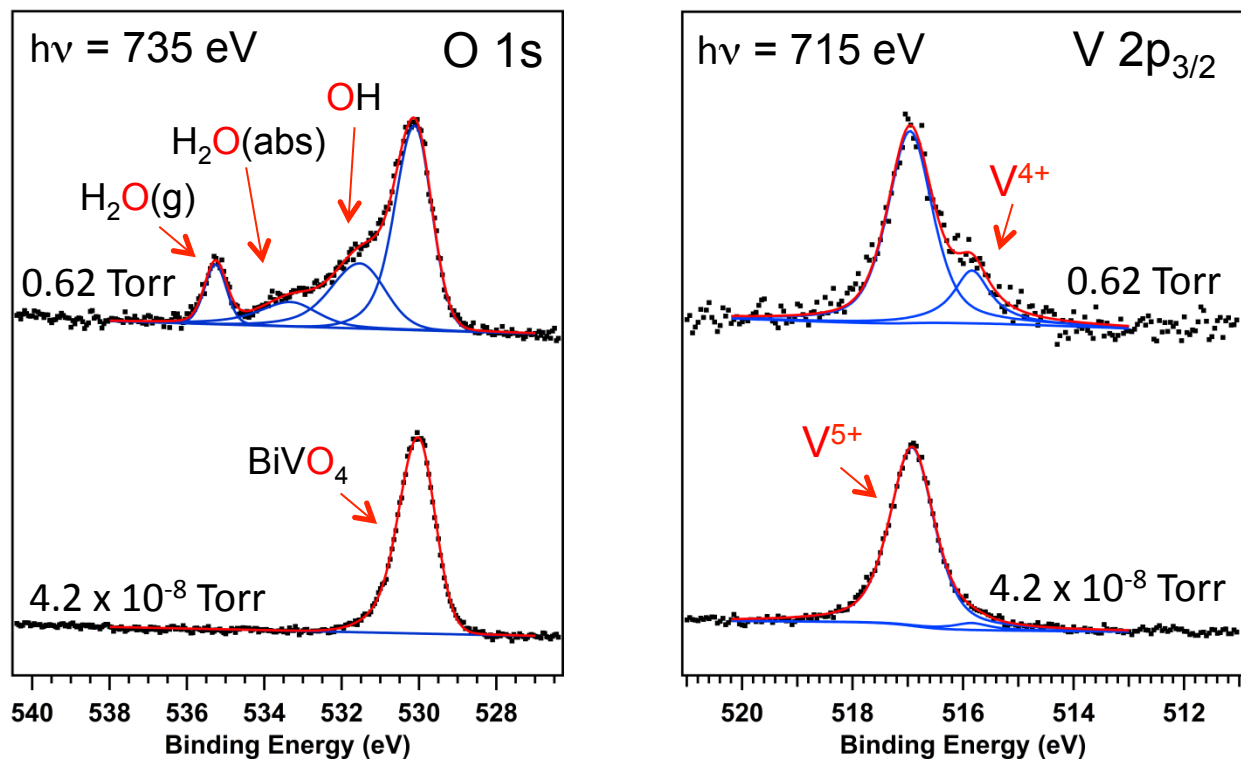
Figure 4: O 1s (left) and V 2p (right) spectra of a $BiVO_4(010)$ surface in ultra-high vacuum conditions and in 0.62 Torr of water vapor pressure. O 1s contributions from the $BiVO_4$, adsorbed OH, adsorbed H_2O and gas phase water are indicated. At 0.62 Torr of water vapor pressure there is a significant amount of reduced V (V^{4+}) in the surface.
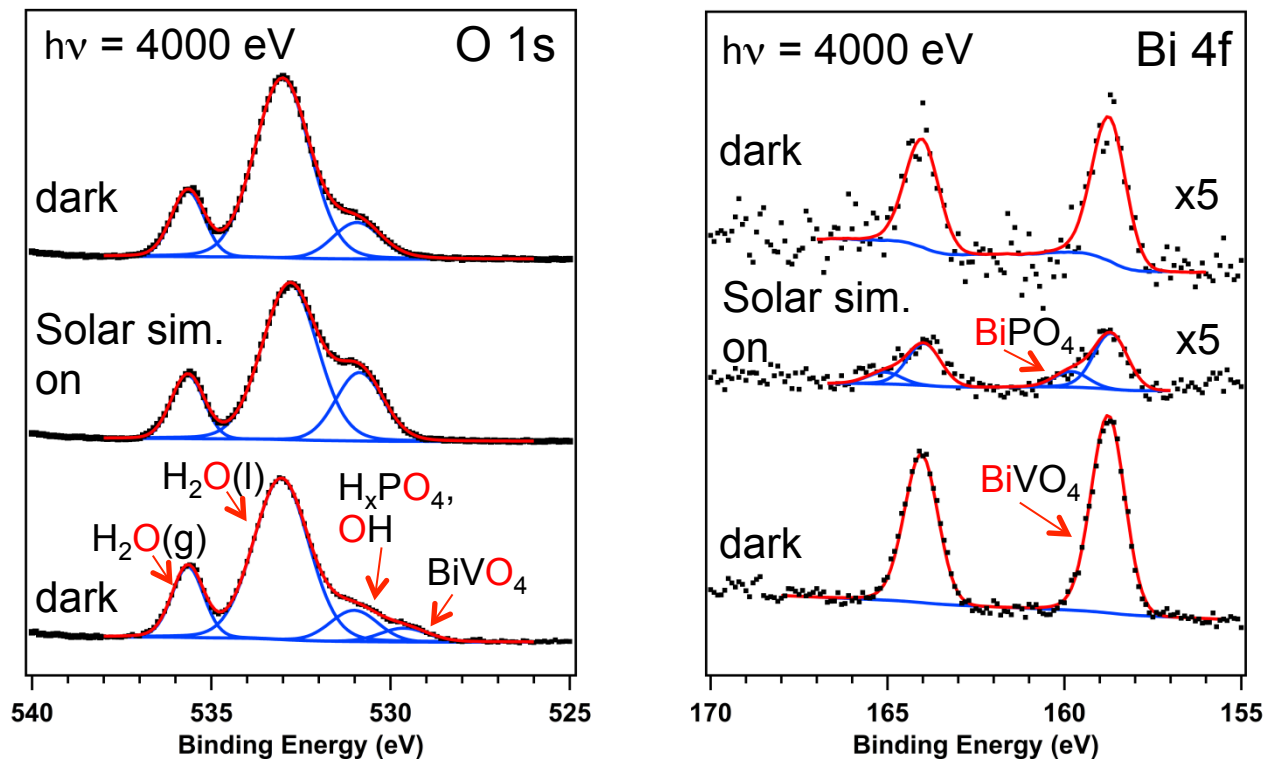
Figure 5: O 1s (left) and Bi 4f (right) spectra of a $BiVO_4$ thin film on FTO/glass under a an approximately 21 nm thick potassium phosphate electrolyte at open circuit potential. The bottom spectra are taken in the dark, the middle spectra are taken after turning on a solar simulator and the top spectra after returning to dark conditions. In the O 1s spectra an increase in the phosphate ions plus OH ion to liquid water signal ratio is observed when the solar simulator is on. In the Bi 4f spectra a broadening to higher binding energy is observed with the solar simulator on.